Optimal Energy Planning for Wireless Self-Contained Sensor Networks in Oil Reservoirs

Abdallah A. Alshehri, Shih-Chun Lin, and Ian F. Akyildiz
Broadband Wireless Networking (BWN) Laboratory
School of Electrical and Computer Engineering
Georgia Institute of Technology, Atlanta, GA 30332, USA
Email: {aalshehri9, slin88, ian}@ece.gatech.edu

***Abstract*—In-situ monitoring of oil reservoirs is crucial for determining the sweet spot of oil and natural gas reserves. Wireless sensor nodes are a promising technology to collect data from oil reservoirs in real time, such nodes are not sufficient for transmitting the required data within a power budget because of limitations caused by the very small size of sensors and the environment. To overcome limitations caused by harsh environmental conditions and power constraints, this paper proposes an accurate energy model framework of a linear oil sensor network topology that gives feasible sensors' transmission rates and sensor network topology while always guarantees enough energy. Since the magnetic induction communication channels is employed, we first examine the non-flat MI fading channels to obtain the accurate received signal qualities. Then, we design MI-based modulation and error control coding schemes and evaluate the energy consumption for MI transmissions to determine optimal sensors' transmissions rate and number of sensors while sensors' packet error rate and energy constraints are satisfied at the same time. we confirm the accuracy of our model via theoretical and simulation evaluations.**

I. Introduction

Unbridled growth in the developing world is increasing global demand for energy. By 2050, oil is projected to comprise over 50% of the total global energy consumption [1]. However, the oil in reserves is diminishing at a rapid pace. Further exacerbating the global energy crisis, the current achievable oil recovery rate, which is the ratio of recoverable oil to total oil in the reservoirs, is less than 60% despite the use of state-of-the-art extraction technologies [2]. Hence, to guarantee global energy security, we must increase the current oil recovery factor. An increasing recovery factor requires the optimal development of oil/gas fields and the optimal management of the recovery process, both of which necessitate real-time and high-resolution physical/ chemical information such as pressure, temperature, and fluid type of the entire oil reservoir. A more thorough understanding of such information could help us significantly increase the recovery factor.

The remote monitoring system [3] and intra-wellbore monitoring systems [4] are not able to measure data deep inside oil reservoirs, and no existing technology has been able to provide real-time and in-situ monitoring of oil reservoirs [5]. However, in-situ sensing techniques for collecting information throughout reservoirs have drawn a great amount of attention from industry and the research community. Currently, most efforts have been devoted to the development of small and compatible sensors that can stand the severe oil reservoir environment [2]. Such wireless sensor nodes have been successfully injected into oil reservoirs [6], as shown in figure 1, depicting a typical oil reservoir environment with a hydraulic fracture. Oil is extracted from a wellbore drilled into underground oil reservoirs at a depth of around 7,000 feet, and hydraulic fracturing is used to make a thin crack inside the rock formation to access more oil and natural gas. To deploy wireless sensor nodes in fractures during the hydraulic fracturing process, we need to address the research challenges of existing wireless sensor networks (WSNs): extremely high path loss, infeasibility of radiating wireless signals, and a prohibitively short system lifetime [7].

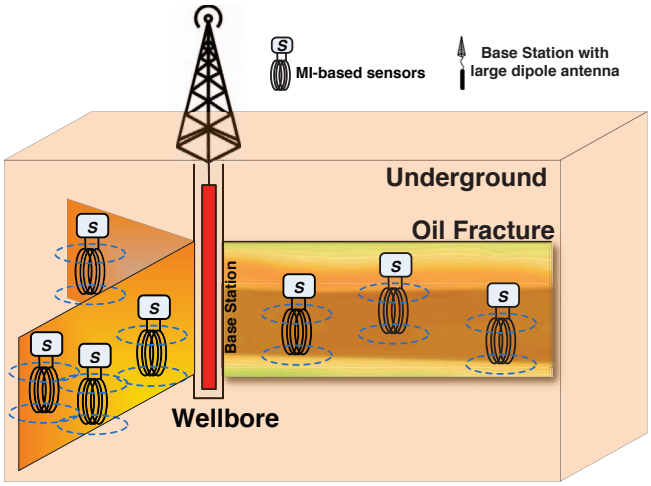

Fig. 1: The system architecture of the MI-based sensor network inside oil reservoir

To overcome the underground oil reservoirs challenges, WSNs based on the magnetic induction (MI) technique was proposed in [8]. Classical electromagnetic (EM) waves cannot work properly in the underground oil reservoir environment. This oil environment consist of crude oil, gas, soil and rocks which are very significant material absorptions for EM waves. Consequently, the path loss in such environment is excessively high resulting in extremely short communication

978-1-4673-8999-0/17/$31.00 ©2017 IEEE

range, unreliable channel conditions, and large antenna sizes which is very crucial element in underground sensor nodes. In order to use very small antenna, the EM waves need to radiate over a frequency of hundreds of GHz or several THz. The propagation of such high frequency signals in the oil reservoirs is very difficult [7]. The unreliable channel brings design challenges for the EM-based sensor nodes and networks to achieve both satisfying connectivity and energy efficiency. These challenges prevent using EM-based WSNs in the underground oil reservoirs.

Instead of using EM waves, the alternative solution is the MI technique which enables wireless communication in the underground oil reservoirs and deals with the underground challenges. It transmits the data over the near magnetic field of antennas resulting in achieving constant channel conditions using small size antennas. These special characteristics prompt the MI communication in underground oil reservoir environments. In our case, the sensor nodes use an MI coil antenna to generate and receive wireless signals through magnetic coupling. The near magnetic field generated by the MI coil can efficiently penetrate a high-loss oil reservoir channel and realize the wireless communication [9]. It should be noted that the power issue is extremely critical for sensors in oil reservoirs. The capacity of transmitting sensing data depends on the harvested energy. Once the senors are injected into a fracture, they cannot be replaced. Thus, we need to address and analyze an accurate energy model to ensure sufficient power to sensor nodes inside oil reservoirs and to enable real-time monitoring by sensor networks.

In this paper, we first investigate MI channel models and physical-layer communication functionalities. Then, we propose an accurate energy planning framework to facilitate self-contained sensor networks in oil reservoirs. Specifically, this framework gives feasible sensors' transmission rates and sensor network topology while always guarantees enough energy for all sensors. To the best of our knowledge, this work is the first to provide optimal energy planning in terms of sensors density and data rates for wireless self-contained sensor networks in challenged oil reservoir environments. The remainder of this paper is organized as follows. Section II introduces the system model of sensor nodes in oil reservoirs, and section III discusses the influence of magnetic-inductive channels on communication functionality in oil reservoirs. Section IV discusses optimal energy planning framework for wireless self-contained sensor networks, and Section V provides numerical results. Section VI summarizes the conclusions.

II. System Model

In this section, we explain the system model for oil reservoirs wireless sensor network and the energy consumption and harvesting model of the entire sensor network system. Figure 1 illustrates the system architecture of the MI-based sensor network, which has two layers:

1) **Sensor nodes** in the oil-fractured reservoir, which are injected into the fracture during the hydraulic fracturing process. Since the fracture is very thin, their positions are randomly distributed and linear inside the fracture. The wireless sensor nodes have no power source, but they are wirelessly charged by the radiation of the base station inside the wellbore.
2) **A base station**, which consists of a large antenna at the wellbore connected to an aboveground gateway.

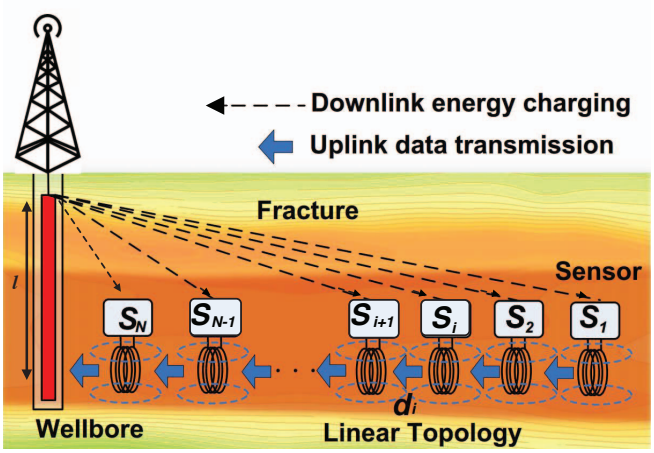

Fig. 2: The network topology of the MI-based sensor network inside the oil fractured reservoirs

A. Linear Network Topology in Oil Reservoirs

The oil reservoir's fractures characteristics determines the network topology. Fractures, which average 0.01 m wide and 1 m high, can reach up to 100 m long. Based on the fractures characteristics, The positions of the sensors are random, static, and linear inside the fracture. Thus, we assume a static linear topology for the wireless sensor network inside the fracture as illustrated in figure 2, which shows that energy is transferred and harvested in a one-hop energy fashion while data are transmitted in a multi-hop fashion. According to the system architecture described previously, we propose a three-stage operational structure as follows:

1) A one-hop radiative energy charging stage in which the base station radiates energy into a fracture and communicates with the sensor nodes. The base station is located at the wellbore and equipped with very high transmission power antenna which allows the usage of MHz frequency to radiate EM signals and transfer the energy through the oil reservoir medium to the MI sensor nodes distributed in the oil-fractured reservoir.
2) A multi-hop MI-communications stage in which the sensor nodes utilize the MI communication mechanism to transmit the sensed data to the nearest neighbor node, and by consecutive relaying, the multi-hop transmission route is used to transmit the data back to the base station. The sensor nodes have no self-power source but harvest energy from EM radiation by the base station. It should noted that the sensor nodes will not operate until they collect sufficient energy.
3) A backbone communications stage in which the base

station receives the sensed data from the sensor nodes in the fractures and then forwards the data through an above-ground gateway.

B. Energy Consumption and Energy Harvesting for Wireless Self-Contained Sensor Networks

The downlink energy charging operates in one-hope fashion to charge the entire sensor network. Due to the very narrow fracture, the size of sensor nodes is extremely small which limits the battery capacity. Consequently, the small battery cannot store enough power for the sensors to perform the communication and sensing functionalities. Due to this limitation, the battery is replaced by ultra-capacitor to store the harvested energy for the sensor operations. Accordingly, it is very crucial to obtain accurate energy charging and consumption model since the capacity of transmitting sensed data depends on the harvested energy. From the channel models obtained in [8], the base station antenna generates an EM field in the MHz frequency range to transfer energy and transmits data to the sensor nodes in the fracture. The EM field will be influenced by inhomogeneous environment, and various fluids, such as crude oil and proppants inside the fracture. The main materials outside of the fracture are soil and rock, as shown in Fig 1. As a result, the liquids and materials affect the path loss of downlink channels accordingly. Hence, a balance between transferred energy and consumed energy is mandatory in order to enable the entire sensors network to perform all the sensing activities and rely the data to the base station.

III. Influence of Magnetic-Inductive Channels on Communication Functionality

To support reliable MI transmissions in underground, the peculiarity of MI communication channels (i.e., non-flat fading in frequency response) should be investigated in detail. In this section, we first examine the non-flat MI fading channels to obtain the accurate received signal qualities. Based on these, we design MI-based modulation and error control coding schemes and evaluate the energy consumption for MI transmissions.

A. Non-Flat Magnetic Inductive Fading Channels

As magnetic induction serves as a feasible solution for underground communication [8], a careful examination for its peculiar channel response is needed. First, as shown in figure 3, coil antennas are used as the front-ends for MI transmissions among sensors, and the near-magnetic field of coils are employed to disseminate the information. Our previous work [8] shows that MI communication encounters less channel variations than the EM waves, where the undesired noise, mainly from the thermal vibration of circuit elements, lets Additive White Gaussian Noise (AWGN) to be applicable as an accurate assumption for the channel. Specifically, the received MI signal can be formulated as

$$r(t) = s(t) * h(t) + n(t) \tag{1}$$

where $s(t)$ denotes the transmitted signals from a sensor transmitter, $h(t)$ denotes the impulse response of the MI channel, and $n(t)$ is for environmental noise. Second, through the matched filter design for MI receiver architecture, shown in figure 3, the received MI symbols are calculated as

$$\begin{aligned} r_k &= \int_0^T [s(t) * h(t)] f_k(t) dt + \int_0^T n(t) f_k(t) dt \\ &\triangleq s_k + n_k, \ 1 \le k \le n \end{aligned} \tag{2}$$

where n_k is a Gaussian random variable with zero mean and $N_0/2$ variance and f_k corresponds to the kth operating frequency. It implies that the mean and variance of received MI symbol r_k are respectively

$$E[r_k] = s_k \ \text{ and } \ \delta_{r_k}^2 = \delta_{n_k}^2 = \frac{1}{2} N_0. \tag{3}$$

These values will be used to calculate the energy consumption of MI transmissions in later sections. In addition, with the aid of the transformer model for MI-based transceivers in *general* underground settings from our previous study [10], we are able to accurately characterize the channel response $H^{MI}(f)$ for MI-based transmissions in *specific* oil reservoirs.

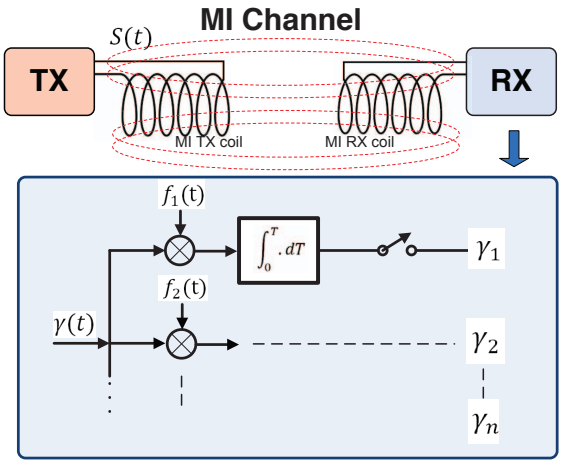

Fig. 3: Front-ends and receiver architecture for MI communication.

Figure 4 shows the frequency response and 3-dB bandwidth of MI channels in oil reservoirs. Specifically, through precise parameter settings for oil reservoirs, the results indicate that the transmission bandwidth of this MI system is still around 1 KHz (as similar to the case in general underground environments in [10]) with 10 MHz operating frequency. The 1 KHz transmission bandwidth will be enough for the specific applications of oil reservoir sensing and monitoring. Moreover, in this bandwidth, the MI channel response lies non-flat, which significantly affect the received signal qualities and the designs of communication functionalities. In the following, we consider this effect in modulation and error coding scheme.

B. Magnetic Inductive-Based Modulation and Error Control Coding

Based on our previous study [10], complicated modulation techniques cause more energy consumption and are not recom-

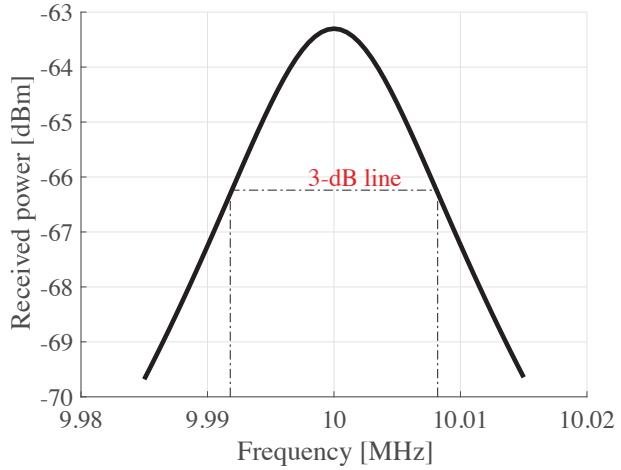

Fig. 4: Frequency response $H^{MI}(f)$ of MI channels in oil reservoirs.

mended for energy-constraint underground sensor networks. To this end, we select two simple but suitable modulation schemes, BPSK and 16-QAM, for our specific application of oil reservoirs. Moreover, due to the non-flat MI channel response, we jointly consider the power spectral density (PSD) of modulated signals and the channel response, when evaluating received signal strengths and bit error rates (BERs). The details are given as follows.

Assume the rectangular shaping pulse is adopted for MI-based transmissions. The PSD for PSK and QAM modulations can be obtained as follows:

$$\begin{aligned} PSD_{PSK}(f) &= A^2 T_s \delta_r^2 (\tfrac{sin(\pi f)T_s}{\pi f T_s})^2; \\ PSD_{QAM}(f) &= A^2 T_s \delta_r^2 (\tfrac{sin(\pi f)T_s}{\pi f T_s})^2, \end{aligned} \tag{4}$$

where T_s denotes the symbol duration, A and δ_r^2 denotes the magnitude and the variance of MI signals, respectively. Let E_b^{MI} and E_s^{MI} be the received energy of one bit and one symbol over MI channels, respectively. This implies that $E_b^{MI} = E_s^{MI}/\log_2 M$ for MQAM modulation. Hence, given E_s as the energy of transmitted signal $s(t)$, we obtain the received energy under modulation scheme x as

$$E_s^{MI} = E_s \frac{\int^{BW} PSD_x(f) H^{MI}(f) df}{\int^{BW} PSD_x(f) df}. \tag{5}$$

This implies that in order to capture the non-flat fading effect, the equivalent energy loss due to MI transmissions has more complicated form (i.e., through the integration over the product of signal PSD and channel response). Figure 5 shows a case study for 16-QAM modulated MI signals. The results indicate that as the feasible transmission bandwidth is small (i.e., around 1 KHz) for MI communication, the signal PSD can be seen as a constant in this bandwidth, which will be true for most of widely-used modulation schemes. Hence, the energy calculation in Eq. (5) will be greatly simplified. Finally, with

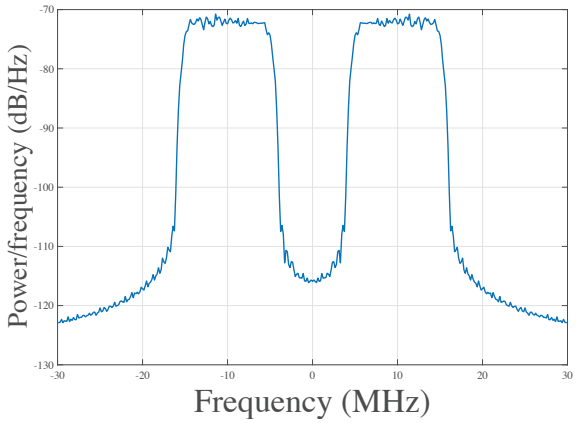

(a) The PSD of the modulated signal.

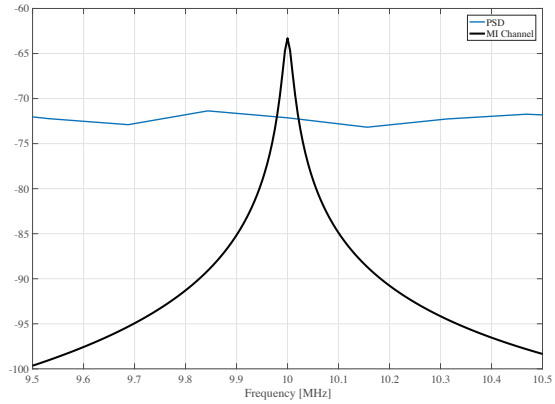

(b) The comparison of frequency response and PSD.

Fig. 5: Frequency response $H^{MI}(f)$ of MI channels and the PSD of the 16-QAM modulated MI signal.

above accomplishments, we can obtain the BER for BPSK and MQAM modulated MI signals, respectively, as

$$\begin{aligned} \xi^{PSK} &\cong Q\left(\sqrt{\tfrac{2E_b^{MI}}{N_0}}\right); \\ \xi^{MQAM} &\cong \tfrac{4}{\log_2 M}(1 - \tfrac{1}{\sqrt{M}}) Q\left(\sqrt{\tfrac{3\log_2 M}{M-1} \times \tfrac{E_b^{MI}}{N_0}}\right). \end{aligned} \tag{6}$$

We further consider the MI-based channel coding as follows. Specifically, automatic repeat request (ARQ) requires timeouts and acknowledgements, which are great overheads for energy-limited underground sensor networks. Hence, we select forward error correction (FEC) to enhance link transmission reliability. In particular, multilevel cyclic BCH (Bose, Ray-Chaudhuri, Hocquenghem) codes are preferred, because of its energy-efficiency as compared to convolutional codes [11]. To this end, we adopt BCH codes $BCH(n, k, t)$ with rate $R^C = k/n$ in our work, where n denotes the block length, k denotes the payload length, and t denotes the correcting capability of bit error (i.e., $t < n$). Specifically, given the BER ξ from Eq.(6) and L[bit] as the packet length, the packet error rate (PER) Φ_i for the data transmissions

between sensors x_i and x_{i+1} is obtained as

$$\Phi_i(d_i) = 1 - [1 - \sum_{j=t+1}^{n} \left(\begin{array}{c} n \\ j \end{array} \right) \xi_i^j (1-\xi_i)^{n-j}]^{\lceil \frac{L}{k} \rceil}. \quad (7)$$

where d_i denotes the distance between sensors x_i and x_{i+1}. This PER can be further approximated as

$$\Phi_i(d_i) \approx \lceil \frac{L}{k} \rceil \sum_{j=t+1}^{n} \left(\begin{array}{c} n \\ j \end{array} \right) \xi_i^j (1-\xi_i)^{n-j}. \quad (8)$$

As a result, to establish reliable MI communication, we formulate the end-to-end (i.e., from a sensor to the BS in the wellbore) PER constraint as follows: for sensor $x_i, i \in N$ with i hops to the BS in the linear topology,

$$1 - (1 - \Phi_i(d_i))^i \leq \Phi_T^{e2e}, \quad (9)$$

where Φ_T^{e2e} is a given tolerable maximum end-to-end PER. It implies the end-to-end PER should be no greater than the given tolerable value. Upon this stage, we have completed the study of non-flat fading effect in modulation and channel coding designs.

Energy consumption for MI transmissions: Based on the energy modeling in Eq. (5), we are able to characterize sensors' energy consumption from uplink data transmissions. Specifically, the energy consumption per bit for sensor $x_i, i \in N$ with MQAM can be modeled as follows:

$$\frac{E_s}{\log_2 M} + 2E_b^{elec}, \quad (10)$$

where E_b^{elec} is from the required energy per bit by the transmitter and receiver electronics (e.g., PLLs, bias current, etc.) This will be incorporated in our energy planning framework in Section IV.

IV. Optimal Energy Planning Framework for Wireless Self-Contained Sensor Networks

In this section, based on the detailed examination of MI channels and physical-layer communication functionality, we propose an accurate energy planning framework to facilitate self-contained sensor networks in oil reservoirs. Specifically, this framework gives feasible sensors' transmission rates and sensor network topology while always guarantees enough energy for all sensors. That is, we formulate the optimization problem of optimal energy planning as follows:

[Optimal Energy Planning.]

$$\max_{\{\lambda_i\},N} \quad \sum_{i=1}^{N} \lambda_i \quad (11a)$$

$$\text{s.t.} \quad 1 - (1 - \Phi_i(d_i))^i \leq \Phi_T^{e2e}, \ \forall i \in N; \quad (11b)$$

$$\sum_{j=1}^{i} \lambda_j R_j^C (E_b^{MI}(d_j) + 2E_b^{elec}) \leq E_i^h, \ \forall i \in N \quad (11c)$$

where E_i^h and λ_i denotes the harvested energy (from a stable energy source of the BS) by and the transmission rate of sensor x_i, respectively. The objective function in Eq. (11a) gives the total transmission rate for all N sensors. The constraint in Eq. (11b) is from the consideration of reliable MI transmissions for all sensors (i.e., applying Eq. (9) for all $x_i, i \in N$.) Also, the constraint in Eq. (11c) implies that the consumed energy due to data transmissions by a sensor should be no greater than the harvested energy by that sensor. Therefore, this optimization problem will determine the optimal sensors' transmissions rate and the optimal number of sensors, while satisfy sensor's PER and energy constraints at the same time.

To characterize the energy harvesting (i.e., $E_i^h, \forall i \in N$) from the BS in the wellbore, we adopt the recent results for a energy transfer model in [12]. Specifically, given d as the distance from the BS to a specific sensor, the corresponding path loss for this downlink channel can be formulated as

$$L_{DL}(d) \approx -10 \lg \left\{ \frac{A_1 + A_2 d^2}{d^4} e^{-A_3 d} \right\}, \quad (12)$$

where $A_1 = \frac{N^2 w^2 \mu_2^2 l^2 r^4 k_2^2 sin^2\theta}{64 R_c R_i k_1^2}$ and $A_2 = \frac{N^2 w^2 \mu_2^2 l^2 r^4 k_2^2 sin^2\theta}{64 R_c R_i}$ are the parameters related to the environments (i.e., the fracture) and coil antenna designs, and $A_3 = 2/\delta$ characterizes the skin-depth effect for underground transmissions. The model parameters are: k_1 is the wavenumber inside the fracture, k_2 is the wavenumber outside the fracture, μ_2 is the effective permeability of the soil and rocks outside the fracture, w is the angular frequency, l is the length of the base station antenna, R_i is the input resistance of the base station antenna, d is the distance between the base station and the oil mole. R_c is the resistance of the coil (antenna of oil mole), r is the radius of the coil, N is the number of turns of the coil,and θ is the angle of the coil positions. The details can be found in [12]. Moreover, with this path-loss formulation and the linear network topology in figure 2, we formulate the harvest energy by sensor x_i as follows:

$$E_i^h = T_i^c \eta_i P_{TX} L_{DL} \left(\sqrt{l^2 + (\sum_{i=1}^{n} d_j)^2} \right), \quad (13)$$

where T_i^c and η_i denotes the charging time and the energy conversion rate of sensor x_i, and P_{TX} is the transmitted power of the BS. As a result, the formulated energy planning problem in Eq. (11) can be easily solved by commercial software solvers through an exhaustive searching.

Working on the network planning problem of a large number of sensors, system architect often does not require precise values, but rough and meaning results for sensor's transmissions rate and network topology. Towards this, we simplify the formulation in Eq. (11) with the consideration of $\lambda_i = \lambda, d_i = d, R_i^C = R^C, \forall i \in N$ as

$$\max_{\lambda,N} \quad N\lambda$$

$$\text{s.t.} \quad 1 - (1 - \Phi(d))^N \leq \Phi_T^{e2e}; \quad (14a)$$

$$i\lambda R^C (E_b^{MI}(d) + 2E_b^{elec}) \leq E_i^h, \ \forall i \in N. \quad (14b)$$

This problem then can be solved time-efficiently by the proposed Algorithm 1.

Algorithm 1: Fast Optimal Energy Planning.

set $N = 1$;
repeat
  calculate
    $\lambda^N = \min_{i \le N} E_i^h / [iR^C(E_b^{MI}(d) + 2E_b^{elec})]$
  set $N := N + 1$;
until $N > \log_{(1-\Phi(d))}(1 - \Phi_T^{e2e})$;
$N^* = \arg\max_i i\lambda^i$ and $\lambda^* = \lambda^{N^*}$

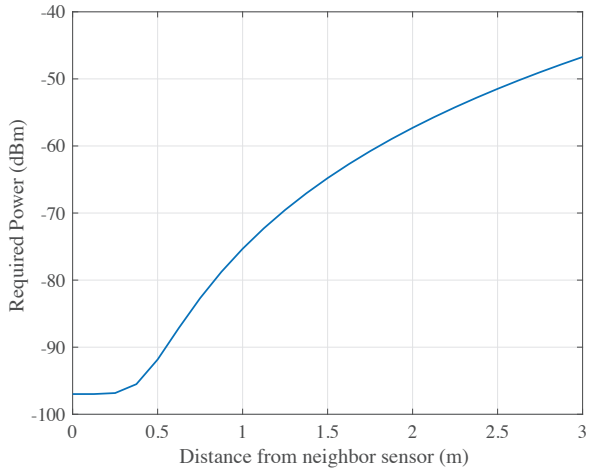

(a) Required power to transmit data from sensor to neighbor sensor

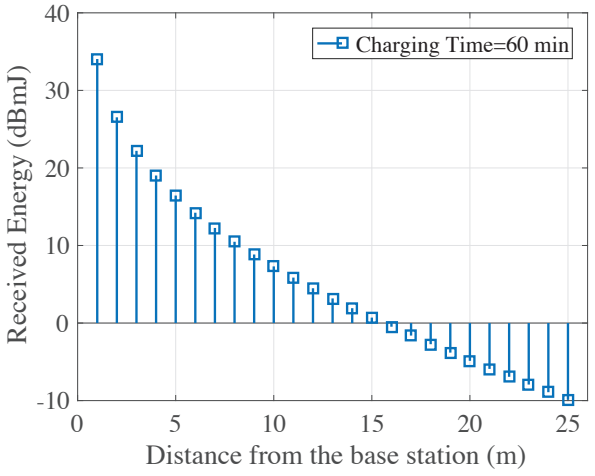

(b) Energy received by sensors from the base station

Fig. 6: Charging and consumed energies in self-contained sensor networks.

V. Numerical Results

This section numerically evaluate the wireless energy charging model and the energy consumption model and points out the effect of bite error rate and packet error rate. It also shows packet error rates for 16QAM and BPSK modulation techniques and for different BCH codes. We set the parameters as follows. The transmission bandwidth is 1kHz, the packet size is 100 bytes, and the operating frequency is 10 MHz.

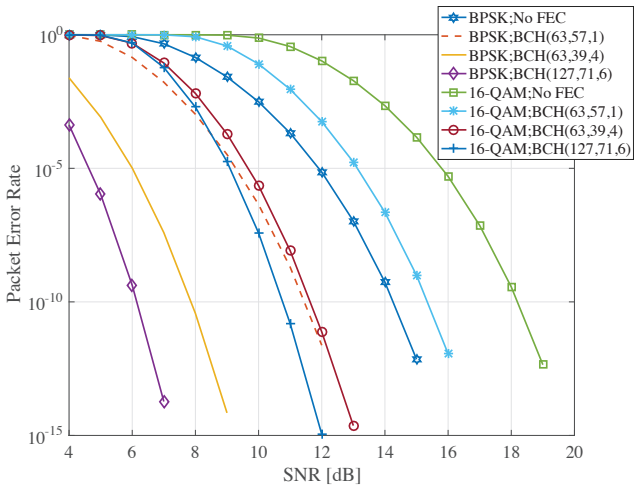

Fig. 7: Packet error rate(PER) vs SNR (dB) for BPSK and 16QAM modulation techniques and BCH(n,k,t) coding schemes.

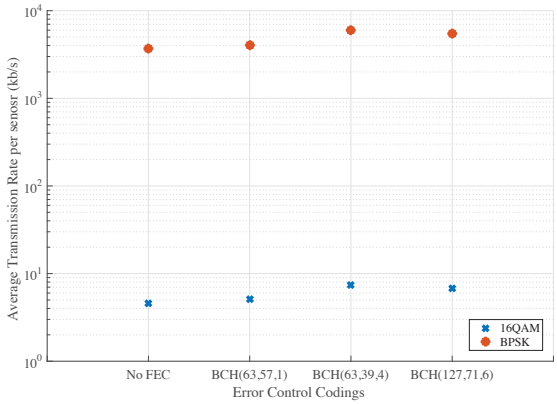

Fig. 8: Optimal transmission rate for BPSK and 16QAM modulation techniques and BCH(n,k,t) coding schemes.

Figure 6a shows the minimum amount of transmission power required to enable inter-sensor communication via the MI channel in oil reservoirs. As the distance between the two sensor nodes increases, the required transmission power also increases dramatically as a result of the complicated transmission medium. Figure 6b shows the harvested energy as a function of the distance between the base station and the sensor nodes in the oil fracture over charging time of 1 hour. The wireless energy charging model shows the power received by the sensor nodes overcoming the oil fracture conductivity constraints. For example, at a 25 m distance from the base station, the harvested energy is around -10 dBmJ, which is enough to charge the ultra-low power MI-based sensor nodes.

Figure 7 shows PER versus SNR for 16QAM and BPSK modulation techniques and for different BCH(n, k, t) codes

and no FEC scheme.The transmission range is set to 2 m and the packet length is set to 100 Bytes. The working temperature is selected as 283 K. While BPSK achieves smaller BER for any given SNR among modulation techniques, it brings the best PER performance for every channel coding schemes. In addition, while consuming more energy to perform, the powerful coding schemes (i.e., with high error correcting capability) keep less PER for any given SNR. A trade-off exists between energy consumption and transmission quality. Figure 8 shows the optimal total transmissions rate of the entire network with respect to different modulation and coding schemes. The total charging time is set to 1 hour. The results implies that BPSK can bring higher transmission rates than 16QAM, regardless of channel coding schemes. Also, in average, 8 Kbps per sensor can be achieved by the investigated modulation and coding.

VI. Conclusion

This paper proposed optimal energy planning of a linear oil sensor network topology that ensures accurate energy model that provides optimal sensors transmission rates and optimal sensor network planning. We showed how the inhomogeneous environment strongly affects the downlink and uplink channels inside oil reservoirs. Since the magnetic induction communication channels is employed, we examined the non-flat fading nature of MI communications to obtain the accurate received signal qualities for reliable MI communications inside oil reservoirs. Then, we designed MI-based modulation and error control coding schemes and evaluated the energy consumption for MI transmissions to determine optimal sensors' transmissions rate and number of sensors while sensors' packet error rate and energy constraints are satisfied at the same time. We also evaluated the modulation and error control coding to transmit data between nodes. We obtained the optimal total transmissions rate of the entire network and number of sensors while sensors PER and energy constraints are satisfied. We confirmed the accuracy of our model via theoretical and simulation evaluations.

Acknowledgement

This work is supported by EXPEC ARC/ Saudi Aramco, Dhahran, Saudi Arabia.

References

[1] Scott Tinker, NSTI Meeting, May 2009, Houston, TX

[2] D. Chapman and W. Trybula, Meeting the challenges of oilfield exploration using intelligent micro and nano-scale sensors, in Proc. 2012 IEEE International Conference on Nanotechnology.

[3] D. L. Gysling and F. X. T. Bostick, Changing paradigms in oil and gas reservoir monitoringthe introduction and commercialization of in-well optical sensing systems, in Proc. 2002 Optical Fiber Sensors Conference Technical Digest, vol. 1, pp. 4346.

[4] O. Duru and R. N. Horne, Modeling reservoir temperature transients, and matching to permanent downhole gauge (PDG) data for reservoir parameter estimation, in Proc. 2008 SPE Annual Technical Conference and Exhibition.

[5] W. C. Lyons and G. J. Plisga, Standard Handbook of Petroleum and Natural Gas Engineering. Gulf Professional Pub., 2005.

[6] Micro sensor motes successfully travel through a canadian heavy oil reservoir. Available: http://www.incas3.eu/news

[7] M. A. Akkas, I. F. Akyildiz, and R. Sokullu, Terahertz channel modeling of underground sensor networks in oil reservoirs, in Proc. 2012 IEEE GLOBECOM.

[8] Z. Sun and I. F. Akyildiz, Magnetic induction communications for wireless underground sensor networks, IEEE Trans. Antennas Propag., vol. 58, no. 7, pp. 24262435, July 2010.

[9] A. K. RamRakhyani, S. Mirabbasi, and M. Chiao, Design and optimization of resonance-based efficient wireless power delivery systems for biomedical implants, IEEE Trans. Biomed. Circuits Syst., vol. 5, no. 1, pp. 4863, Feb. 2011.

[10] S. C. Lin, I. F. Akyildiz, P. Wang and Z. Sun, "Distributed Cross-Layer Protocol Design for Magnetic Induction Communication in Wireless Underground Sensor Networks," in IEEE Transactions on Wireless Communications, vol. 14, no. 7, pp. 4006-4019, July 2015.

[11] Y. Sankarasubramaniam, I. F. Akyildiz, and S. W. McLaughlin, Energy efficiency based packet size optimization in wireless sensor networks, in Proc. IEEE SNPA, Apr. 2003, pp. 18.

[12] H. Guo and Z. Sun, "Channel and Energy Modeling for Self-Contained Wireless Sensor Networks in Oil Reservoirs", IEEE Transactions on Wireless Communications, Vol. 13, No. 4, pp. 2258-2269, April 2014.